Testing the Efficacy of Selected Scalar Parameters for Identifying Ion Diffusion Regions in MMS Data

University of New Hampshire

A.J. Rogers[1], C.J. Farrugia[1], R.B. Torbert[1]

[1]The University of New Hampshire, Department of Physics, Durham, NH

December 10, 2019

Abstract

Canonical parameters for Ion Diffusion Region (IDR) identification such as ion flow reversals or Hall fields rely on the observatory passing through several spatially-separated features in the region surrounding the reconnecting X-line and on the accurate determination of a coordinate system natural to the X-line. Scalar parameters derived from direct field measurements and particle distribution functions do not rely on any particular coordinate system or flight path of the observatory. Examples such as particle agyrotropy and the adiabatic expansion parameter have been suggested to identify or even define the Electron Diffusion Region (EDR) when applied to electron measurements. The same physics is equally applicable to ion diffusion and demagnetization. We present four such parameters, adapted for use with ion measurements, and test their efficacy in identifying IDRs in the geomagnetic tail during the 2017 MMS tail season. We compare them in regions containing known IDRs identified independently using canonical criteria (see Rogers *et al.*, 2019) against regions where no IDRs exist. While no parameter is found to be sufficient for IDR identification, a combination of scalar parameters prove to be moderately effective.

Methodology

Fast survey-level data from MMS is used to calculate each of the parameters for the entire 2017 tail season (May 05 — September 26) where the location of MMS was at least $8R_E$ away from the Earth and where the tetrahedron quality factor (TQF) ≥ 0.8. The amount of time spent in each $\frac{1}{2}R_E \times \frac{1}{2}R_E$ grid square of the geomagnetic tail was then determined and plotted. Each time step was then tested for if **ALL** parameters met or exceeded their threshold values and the amount of time in each grid square where each condition was met was calculated and plotted. Times and locations where all parameters were satisfied have been tabulated and retained for review.

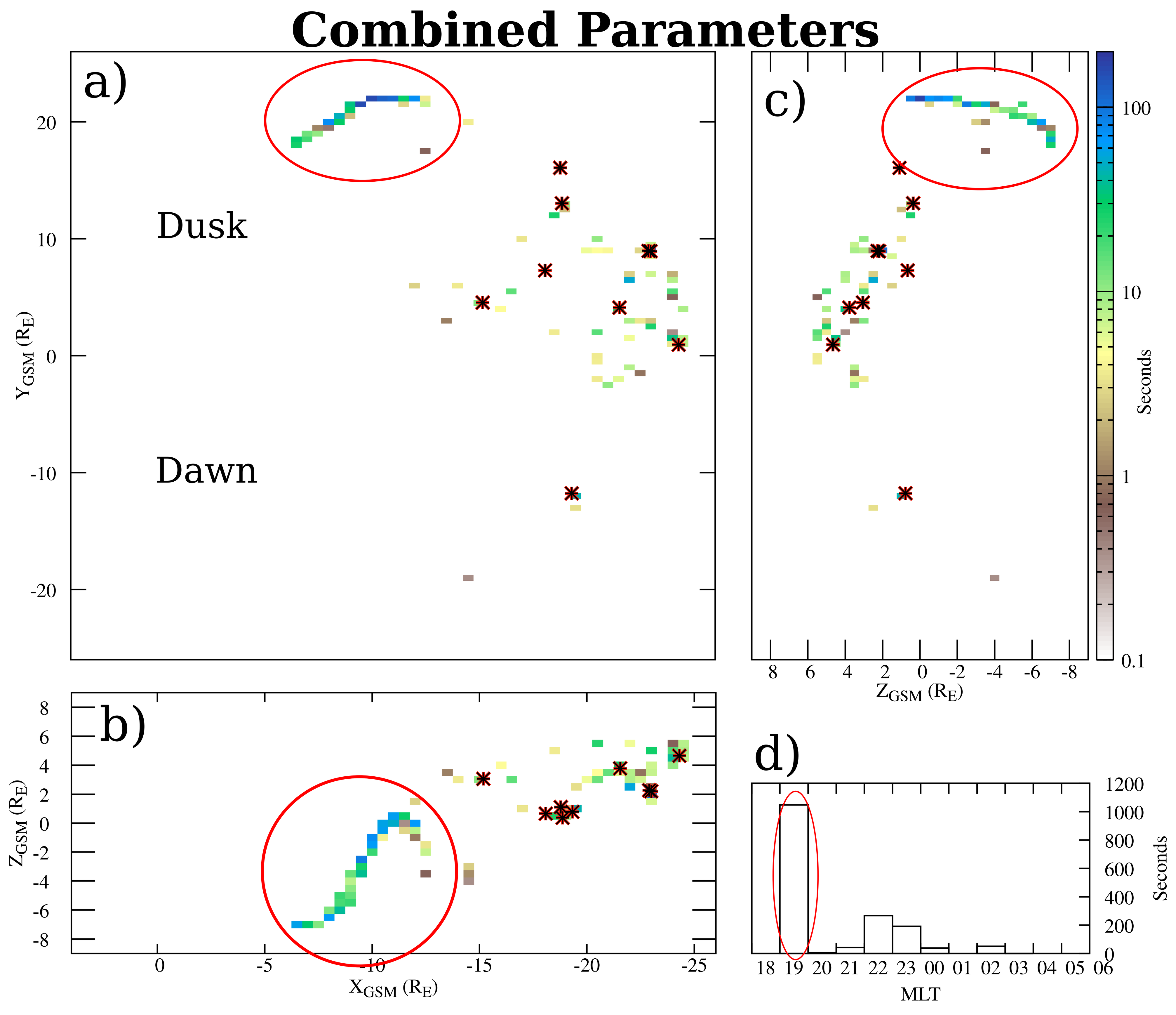

Figure: **1. Combined Parameters**: The dwell time in seconds is shown for each $\frac{1}{2}R_E \times \frac{1}{2}R_E$ grid square of the geomagnetic tail where all of the 4 parameters considered exceeded their threshold values, as observed by MMS. *a)* shows the projection in the $X - Y_{GSM}$ plane; *b* the $X - Z_{GSM}$ plane; and *c)* the $Z - Y_{GSM}$ plane. *d)* shows the total time as a function of MLT. Stars mark previously identified IDRs (Rogers *et al.*, 2019). The red circle highlights the dwell time associated with 2017-09-11 (09:30) — 2017-09-12 (0430) UTC.

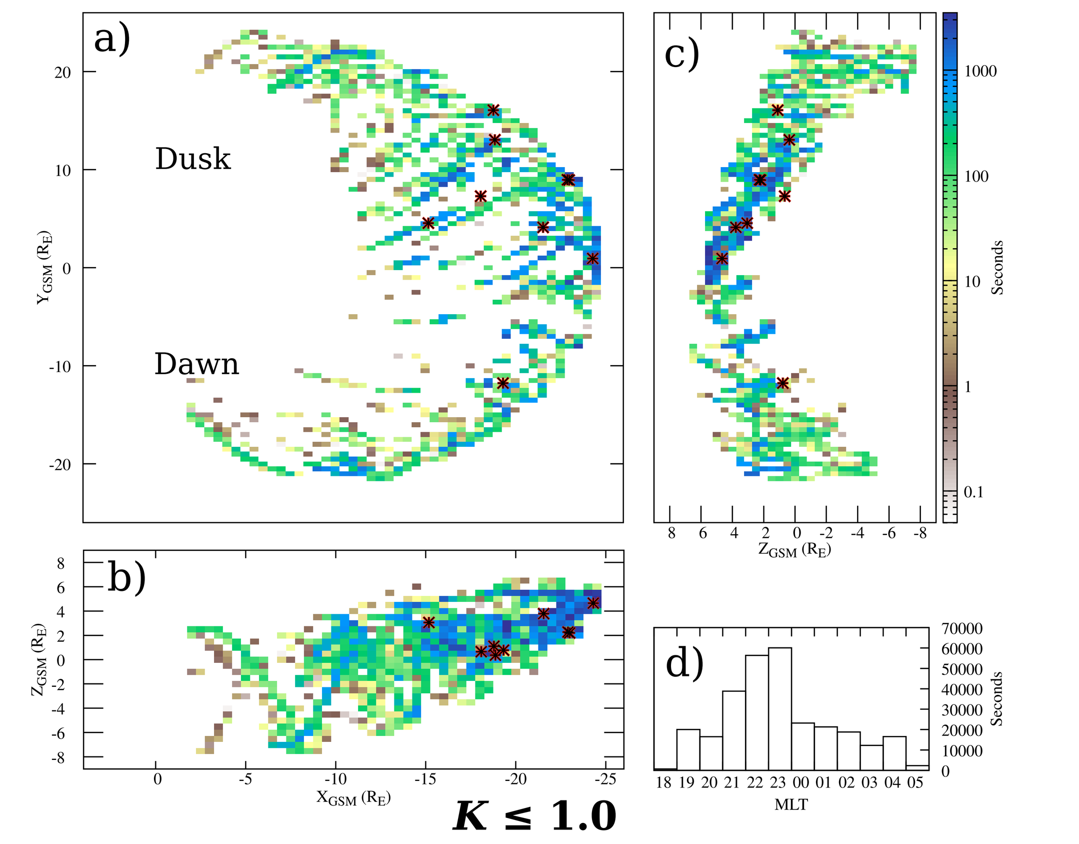

Figure: **2. *K***: the dwell time in seconds where MMS measured $K \leq 1.0$. Subplots are arranged as in Figure 1.

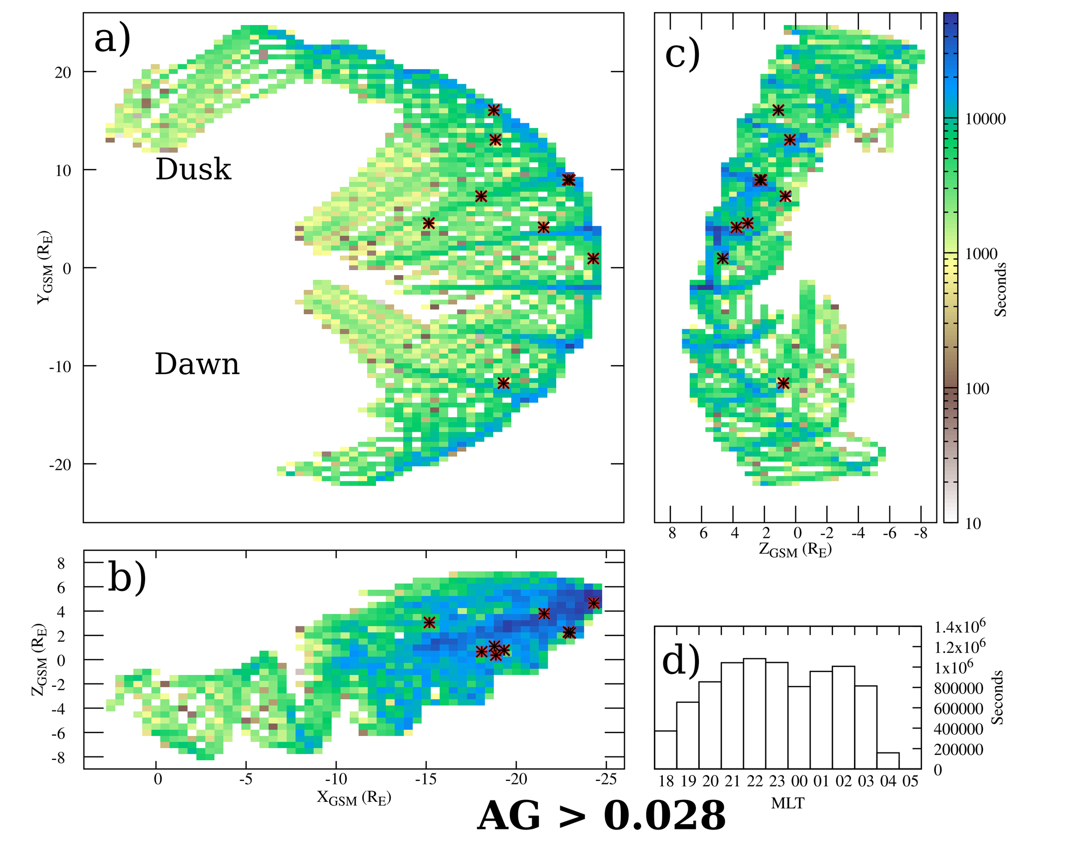

Figure: **4. AG**: the dwell time in seconds where MMS measured $AG \geq 0.028$. Subplots are arranged as in Figure 1.

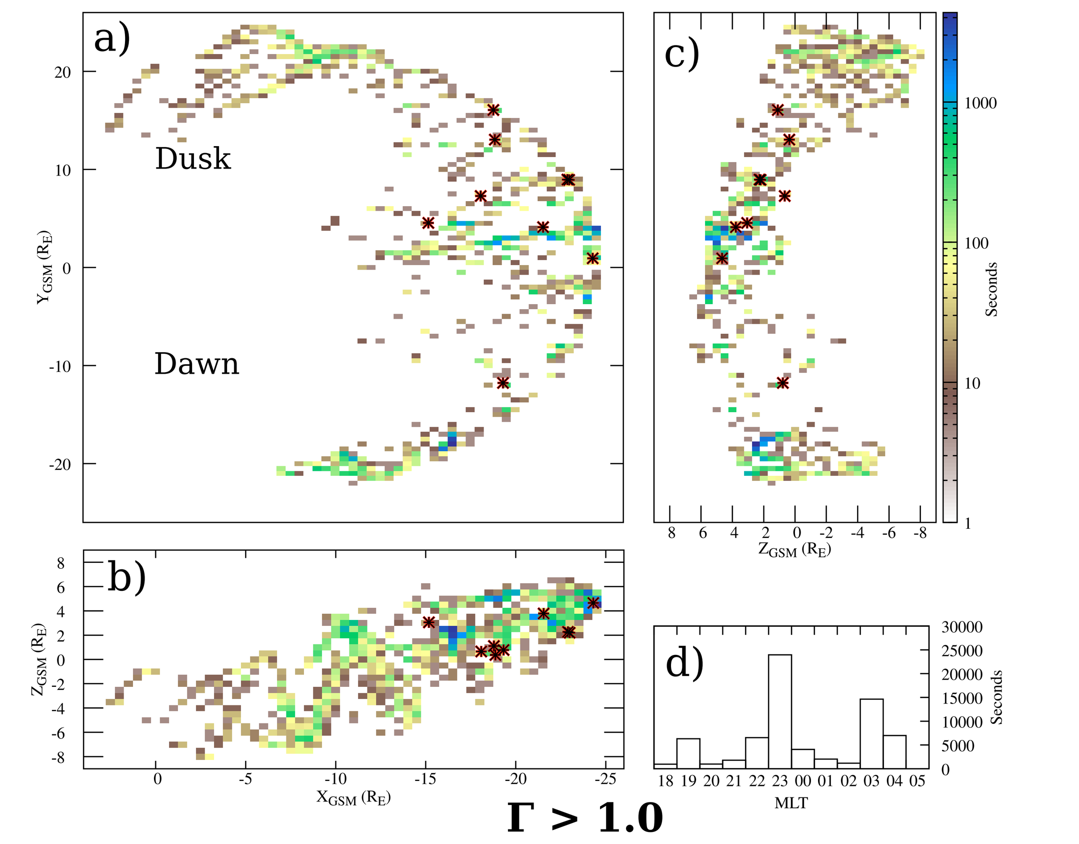

Figure: **3.** Γ: the dwell time in seconds where MMS measured $\Gamma \geq 1.0$. Subplots are arranged as in Figure 1.

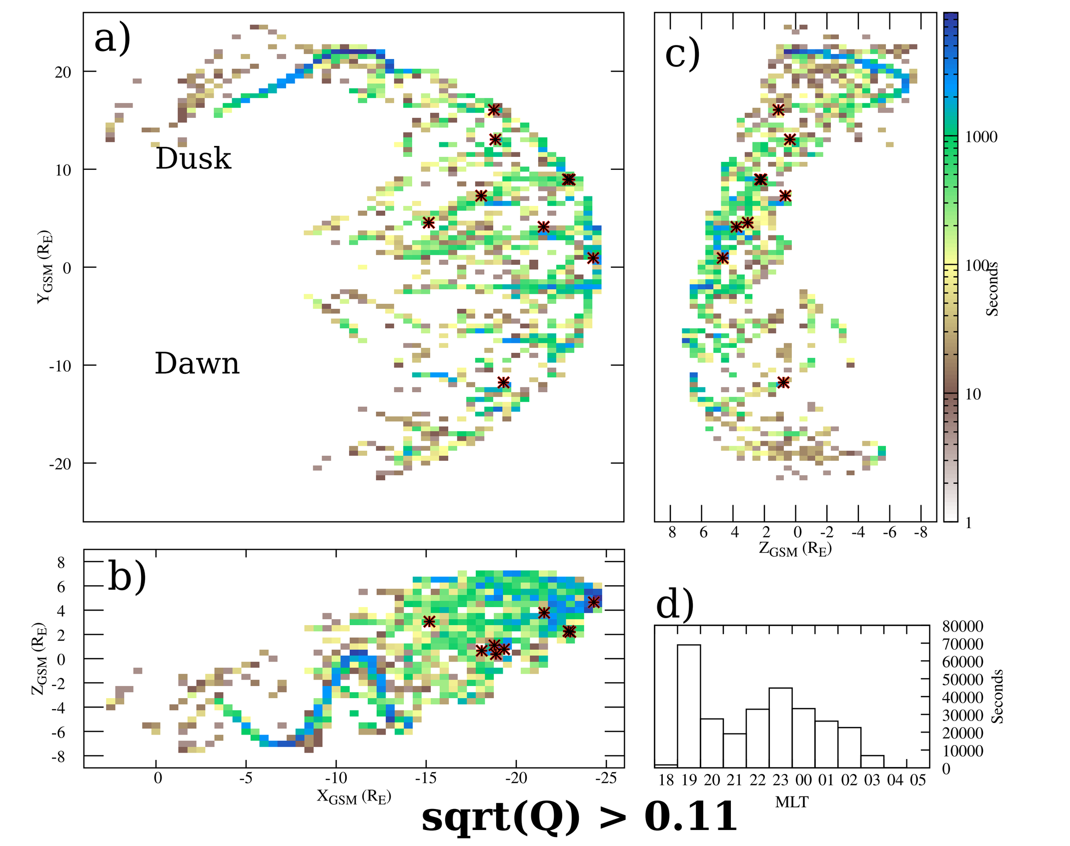

Figure: **5.** $\sqrt{Q}$: the dwell time in seconds where MMS measured $\sqrt{Q} \geq 0.11$. Subplots are arranged as in Figure 1.

Parameters Used

Parameter	Expression
Kappa:K	$K = \sqrt{\frac{R_C}{r_g}}$
Agyrotropy:$\sqrt{Q}$	$Q = \frac{4I_2}{(I_1 - P_\parallel)(I_1 + 3P_\parallel)} : I_1 \equiv \mathrm{Tr}(\bar{P}_i), I_2 \equiv$ sum of principal minors
Agyrotropy:AG	$AG = \frac{\lvert 4\det(\bar{P}) - P_\parallel(\mathrm{tr}(\bar{P}) - P_\parallel)^2 \rvert}{4\det(\bar{P}) + P_\parallel(\mathrm{tr}(\bar{P}) - P_\parallel)^2} : \bar{P} \equiv$ Pressure Tensor
Adiabatic Expansion parameter:Γ	$\Gamma_{\perp,i} = \frac{\lvert \vec{E}_\perp + \vec{u}_i \times \vec{B} \rvert}{w_{\perp,i} B} : w_{\perp,i} \equiv \sqrt{\frac{2K_B T_{\perp,i}}{m_i}}$

Table: **1** List of the chosen diffusion scalar parameters, their expressions in terms of *in situ* measurements.

Conclusions

- No single parameter is sufficient to identify or even significantly filter for IDRs.
- Combining parameters provides a useful filter.
- All previously identified IDRs (Rogers *et al.*, 2019) are captured using combined parameters.
- Regions which satisfy the combined parameters but without previously identified IDRs deserve further study.
- Exceptional orbit on 11—12 September, red circles in Figure 1, not a typical tail IDR but magnetopause dynamic event (dozens of MP crossings).

References

— Bučhner, J., and L. M. Zelenyi. (1987). Chaotization of the electron motion as the cause of an internal magnetotail instability and substorm onset. *J. Geophys. Res. 92(A12).* 13,456. DOI:10.1029/ja092ia12p13456
— Che, H. *et al.* (2018) "Quantifying the effect of non-Larmor motion of electrons on the pressure tensor". *PoP. 25.* DOI:10.1063/1.5016853
— Rogers, A.J, C.J. Farrugia, R.B. Torbert. (2019) "Numerical Algorithm for Detecting Ion Diffusion Regions in the Geomagnetic Tail with Applications to MMS Tail Season May 1- September 30, 2017". *JGR:SP. 124.* DOI:10.1029/2018ja026429
— Scudder, J.D, F.S. Mozer. (2005) "Electron demagnetization and collisionless magnetic reconnection in $\beta << 1$ plasmas". *Physics of Plasmas. 12.* 092903.
— Swisdak, M. (2016) "Quantifying gyrotropy in magnetic reconnection". *GRL. 43.* 43-49.

Acknowledgements

Thanks are owed to: Timothy Rogers, Matt Argall, Akhtar Ardakani, John Marci, Ivan Dors, Christine Schultz, Hiroshi Matsui, Kristoff Paulson, Dominic Payne, Terry Forbes, and Kevin Genestretti.
Thanks to Zach Dykstra and Phil Doroff For computational support. This work has been supported by NASA via contract 499878Q